



Casian, A.I. and Sanduleac, I.I. (2015) Thermoelectric properties of nanostructured tetrathiotetracene iodide crystals: 3D modeling. *Materials Today: Proceedings*, 2 (2). pp. 504-509. ISSN 2214-7853

Access from the University of Nottingham repository:

http://eprints.nottingham.ac.uk/31242/1/A_Casian-Mat.Today%20Proc.%202015%2C2%2C504-509.pdf

Copyright and reuse:

The Nottingham ePrints service makes this work by researchers of the University of Nottingham available open access under the following conditions.

- Copyright and all moral rights to the version of the paper presented here belong to the individual author(s) and/or other copyright owners.
- To the extent reasonable and practicable the material made available in Nottingham ePrints has been checked for eligibility before being made available.
- Copies of full items can be used for personal research or study, educational, or not-for-profit purposes without prior permission or charge provided that the authors, title and full bibliographic details are credited, a hyperlink and/or URL is given for the original metadata page and the content is not changed in any way.
- Quotations or similar reproductions must be sufficiently acknowledged.

Please see our full end user licence at:

http://eprints.nottingham.ac.uk/end_user_agreement.pdf

A note on versions:

The version presented here may differ from the published version or from the version of record. If you wish to cite this item you are advised to consult the publisher's version. Please see the repository url above for details on accessing the published version and note that access may require a subscription.

For more information, please contact eprints@nottingham.ac.uk

12th European Conference on Thermoelectrics

Thermoelectric properties of nanostructured tetrathiotetracene iodide crystals: 3D modeling

Anatolie Casian*, Ionel Sanduleac

Department of Computers, Informatics and Microelectronics, Technical University of Moldova,

Stefan cel Mare av., 168, MD-2004, Chisinau, Rep. of Moldova

Abstract

A more complete three-dimensional (3D) physical model for nanostructured crystals of tetrathiotetracene iodide, TTT_2I_3 , is presented. The restrictions on the thermoelectric figure of merit ZT that this model involves are determined. At the same time, the criteria of application of simplified 1D model are defined more precisely. In TTT_2I_3 crystals the carriers are holes. As earlier, two interaction mechanisms of holes with acoustic phonons are considered, generalized for 3D case. One interaction is similar to that of polaron and other to that of deformation potential. Interaction of carriers with impurities and defects is also taken into account. Along chains (x direction) the transport mechanism is of the band type, but in the transversal directions it is of hopping type. The electrical conductivity σ_{xx} , the thermopower (Seebeck coefficient) S_{xx} , the electronic thermal conductivity κ_{xx}^e and $(ZT)_{xx}$ along the conductive chains have been modelled for the first time in the 3D model. Optimal parameters which predict a considerable increase of $(ZT)_{xx}$ are determined.

© 2014 Elsevier Ltd. All rights reserved.

Selection and peer-review under responsibility of Conference Committee members of the 12th European Conference on Thermoelectrics.

Keywords: Tetrathiotetracene iodide; nanostructured crystals; electrical conductivity; thermopower; thermoelectric figure of merit.

1. Introduction

Organic materials attract more and more attention for thermoelectric applications because they have much more diverse properties in comparison with the inorganic ones and their electronic structure is well tunable through molecular chemistry and doping procedures. Besides, organic materials usually have lower thermal conductivity, can be easier produced, are cost effective and are environmentally friendly. In the past two decades big efforts were

* Corresponding author. Tel.: 37322 509 912; fax: 37322 509 905.

E-mail address: acasian@mail.utm.md

undertaken to investigate the thermoelectric applications of organic materials, especially of conducting polymers (see the review [1]).

Poly(3,4-ethylenedioxythiophene) (PEDOT) doped by poly(styrenesulphonate) (PSS) is promising as an organic-based thermoelectric material due to its stability in air and potential for very high electrical conductivity (measured over $300,000 \text{ Sm}^{-1}$) [2]. By optimizing the carrier concentration a value of the thermoelectric figure of merit $ZT = 0.42$ has been measured in p-type [2, 3] and 0.20 in n-type [4] materials. Thermoelectric modules containing n-p single couples were fabricated by printing [5]. In (PEDOT:PSS) thin films ZT value of 0.31 was achieved at room temperature [6], very good result.

It was demonstrated that the nanocomposites of organic and inorganic components may have better thermoelectric performance than either component [7-9]. And really, the highest value of $ZT = 0.57$ at room temperature was measured in phenyl acetylene-capped silicon nano particles [10]. Different theoretical models have been also developed [11-14] in order to describe the thermoelectric transport in organic materials.

In molecular nanowires of conducting polymers values of $ZT \sim 15$ and of thermoelectric power factor $\sim 5 \times 10^4 \text{ W/m}\cdot\text{K}^2$ at room temperature were predicted [15] in spite of hopping conducting mechanism that usually gives smaller carrier mobility than the band model.

The quasi-one-dimensional (Q1D) organic crystals attract a special attention. Values of $ZT \sim 20$ have been predicted in highly conducting charge transfer organic crystals, if the crystal purity is sufficiently high [16] assuring huge mobilities. These results were obtained in strongly one-dimensional approximation, when the crystal is formed from 1D conductive molecular chains packed into a three-dimensional (3D) structure. In not very pure crystals of tetrathiotetracene-iodide, TTT_2I_3 , grown from

solution [17] with measured electrical conductivity $\sigma_{xx} = 1.8 \times 10^5 \Omega^{-1} \text{m}^{-1}$, Seebeck coefficient $S_{xx} = 39 \mu\text{V/K}$ and thermal conductivity $\kappa_{xx} = 1.0 \text{ Wm}^{-1}\text{K}^{-1}$ along conductive chains $ZT \cong 0.1$ at room temperature was obtained. But in reported stoichiometric crystals [18], grown by gaseous phase method with $\sigma_{xx} = 10^6 \Omega^{-1} \text{m}^{-1}$, a value of $ZT \sim 1.4$ is expected, if the hole concentration is diminished by two times [19]. These results practically coincide in 1D and 2D approximations, because the carrier mobility in these crystals is already limited by scattering on impurities and additional scattering on adjacent chains is negligible.

The aim of this paper is to present a more complete 3D physical model for TTT_2I_3 crystals and to determine the restrictions on ZT which this model will involve. At the same time the criteria of application of simplified 1D model will be defined more precisely. The electrical conductivity σ_{xx} , the thermopower (Seebeck coefficient) S_{xx} , the electronic thermal conductivity κ_{xx}^e and $(ZT)_{xx}$ along the conductive chains (x-direction) in TTT_2I_3 crystals are modeled as function of Fermi energy in the 3D model for the first time. The optimal parameters which predict a considerable increase of $(ZT)_{xx}$ are determined.

2. TTT_2I_3 crystals in 3D approximation

In the TTT_2I_3 crystals the carriers are holes. As earlier, (see [20] for 2D case) two interaction mechanisms of holes with acoustic phonons are considered, generalized for 3D case. One interaction is similar to that of deformation potential, and the other to that of polaron. Interaction of carriers with impurities and defects is also taken into account. Along chains the transport mechanism is of the band type and metallic, because the hole transfer energy $w_1 = 0.16 \text{ eV}$, the conduction band width is about $25 k_0 T_0$ at room temperature T_0 , the hole concentration is $n = 1.2 \times 10^{27} \text{ m}^{-3}$ and the hole-phonon interaction can be considered as small perturbation. Therefore, when transport is studied along chains, it is conveniently to pass from the localized representation to the Bloch one. The physical model is described in the tight binding and nearest neighbors' approximations. In this case the energy of the hole with the 3D quasi-wave vector \mathbf{k} and projections (k_x, k_y, k_z) , measured from the top of conduction band, has the form

$$E(\mathbf{k}) = -2w_1(1 - \cos k_x b) - 2w_2(1 - \cos k_y a) - 2w_3(1 - \cos k_z c), \quad (1)$$

where the axes x, y, z are directed along the lattice vectors $\mathbf{b}, \mathbf{a}, \mathbf{c}$, and w_1, w_2, w_3 are transfer energies of a hole from the given molecule to the nearest one along $\mathbf{b}, \mathbf{a}, \mathbf{c}$, and $w_1, w_2, w_3 > 0$. From the condition of the crystal quasi-one-dimensionality it results that w_2 and w_3 are much smaller than w_1 .

There are 3 branches of phonon dispersion, one is for longitudinal and two other are for bend vibrations. The analysis shows that the latter give small contribution to the electrical and thermal transport and can be neglected. The frequency of longitudinal acoustic phonons is taken in the form

$$\omega_q^2 = \omega_1^2 \sin^2(bq_x/2) + \omega_2^2 \sin^2(aq_y/2) + \omega_3^2 \sin^2(cq_z/2), \quad (2)$$

where ω_1, ω_2 and ω_3 are the limit frequencies for directions x, y, z . Due to the same crystal quasi-one-dimensionality, ω_1 is much bigger than ω_2 and ω_3 . So as the conduction band is not very large, the variation of electron and phonon wave vectors on the whole Brillouin zone is considered.

As earlier, two the most important hole-phonon interactions are taken into account. One interaction is similar to that of polaron determined by induced polarization of molecules. The coupling constant of this interaction is proportional to the mean polarizability of the TTT molecule α_0 . The second interaction is similar to that of deformation potential. Three coupling constants of this mechanism are proportional to the derivatives w'_1, w'_2 and w'_3 with respect to the intermolecular distance of w_1, w_2 and w_3 . The square of absolute module of hole-phonon interaction matrix element $A(\mathbf{k}, \mathbf{q})$ which appear in the expression of scattering probability has the form

$$\begin{aligned} |A(\mathbf{k}, \mathbf{q})|^2 = & 2\hbar/(NM\omega_q) \{ w_1'^2 [\sin(k_x b) - \sin((k_x - q_x)b) + \gamma_1 \sin(q_x b)]^2 + \\ & + w_2'^2 [\sin(k_y a) - \sin((k_y - q_y)a) + \gamma_2 \sin(q_y a)]^2 + w_3'^2 [\sin(k_z c) - \sin((k_z - q_z)c) + \gamma_3 \sin(q_z c)]^2 \}. \end{aligned} \quad (3)$$

Here N is the number of molecules in the basic region of the crystal and M is the mass of TTT molecule. The parameters γ_1, γ_2 and γ_3 have the means of the ratios of amplitudes of first interaction to the second one in the x direction on chains and in transversal directions y, z , respectively

$$\gamma_1 = 2e^2 \alpha_0 / (b^5 w'_1), \quad \gamma_2 = 2e^2 \alpha_0 / (a^5 w'_2) \quad \text{and} \quad \gamma_3 = 2e^2 \alpha_0 / (c^5 w'_3), \quad (4)$$

where e is the carrier charge and α_0 is the mean polarizability of TTT molecule. Note that so as w_1 , w_2 and w_3 are positive and exponentially decrease with the increase of intermolecular distance, w'_1 , w'_2 and w'_3 will be negative, and γ_1 , γ_2 and γ_3 will be negative too.

3. Charge and heat transport

In a weak electrical field and a weak temperature gradient applied along conductive chains the linearized kinetic equation is solved analytically and the electrical conductivity σ_{xx} , the Seebeck coefficient S_{xx} , the electronic thermal conductivity κ_{xx}^e and $(ZT)_{xx}$ can be expressed through the transport integrals R_n as follows

$$\sigma_{xx} = \sigma_0 R_0, \quad S_{xx} = (k_0 / e)(2w_1 / k_0 T) R_1 / R_2, \quad (5)$$

$$\kappa_{xx}^e = [4w_1^2 \sigma_0 / (e^2 T)] (R_2 - R_1^2 / R_0), \quad (ZT)_{xx} = \sigma_{xx} S_{xx}^2 T / (\kappa_{xx}^L + \kappa_{xx}^e), \quad (6)$$

where $\sigma_0 = (2e^2 M v_{s1}^2 w_1^3 r) / (\pi^3 \hbar a b c (k_0 T)^2 w_1^2)$, v_{s1} is the sound velocity along the chains, k_0 is the Boltzmann constant, $r = 4$ is the number of molecular chains through the transversal section of the elementary cell, κ_{xx}^L is the lattice thermal conductivity and R_n are the transport integrals (for more details see [20] for 2D case)

$$R_n = \int_0^2 d\varepsilon \int_0^\pi d\eta \int_0^\pi d\zeta \varepsilon (2 - \varepsilon) n_{\varepsilon, \eta, \zeta} (1 - n_{\varepsilon, \eta, \zeta}) \times \frac{[\varepsilon + d_1 (1 - \cos \eta) + d_2 (1 - \cos \zeta) - (1 + d_1 + d_2) \varepsilon_F]^n}{\gamma_1^2 (\varepsilon - \varepsilon_0)^2 + D_0 + \{d_1^2 (1 + \gamma_2^2 + 2 \sin^2 \eta - 2 \gamma_2 \cos \eta) + d_2^2 (1 + \gamma_3^2 + 2 \sin^2 \zeta - 2 \gamma_3 \cos \zeta)\} / (8\varepsilon (2 - \varepsilon))} \quad (7)$$

Here $n_{\varepsilon, \eta, \zeta}$ is the Fermi distribution function in the variables $\varepsilon = (1 - \cos(k_x b))$, $\eta = k_y a$ and $\zeta = k_z c$, $\varepsilon_F = E_F / 2w_1$ is the Fermi energy for the 1D case in the unities of $2w_1$, $\varepsilon_0 = (\gamma_1 - 1) / \gamma_1$ is the dimensionless resonance energy in the relaxation time in the same units, $d_1 = w_2 / w_1 = w'_2 / w'_1$, $d_2 = w_3 / w_1 = w'_3 / w'_1$. At room temperature the effect of scattering on static impurities and defects can be estimated in Eq. (7) by a constant D_0 which depends on impurity and defect concentrations and can be made very small, if the crystal purity is rather high.

Because we study the transport at room temperature, we have considered scattering processes elastic and have also neglected in the law of energy conservation during the carrier scattering the contributions of terms containing w_2 and w_3 in comparison with the kinetic energy along the chain, so as w_2 , w_3 are much smaller than w_1 .

In order to determine the parameters d_1 and d_2 we have calculated σ_{yy} and σ_{zz} , and by comparing the calculated data with the experimental one, have established the values of d_1 and d_2 . However, in the transversal y and z directions w_2 and w_3 are much smaller than w_1 , as it was mentioned above. Therefore, for the calculation of σ_{yy} and σ_{zz} the representation of localized states at TTT molecules is used instead of Bloch representation for the calculation of σ_{xx} . The carrier kinetic energy in these directions is much smaller than the hole-phonon interaction energy. Respectively, a canonical transformation has been applied which allows to consider the main part of hole-phonon interaction in the zero approximation. As a result, the carriers in transversal directions become small polarons, the transport mechanism becomes of hopping type and the conductivity – thermally activated. Electrical conductivities σ_{yy} and σ_{zz} have been calculated numerically. From experimental data $\sigma_{yy} \sim \sigma_{zz} = 330 \Omega^{-1} \text{m}^{-1}$ it was found that the hole transfer energies in y and z directions are $w_2 = w_3 = 0.015w_1$. The values w_2 and w_3 are the same because the respective lattice constants are very close: $a = 18.35 \text{ \AA}$, $c = 18.46 \text{ \AA}$. In Ref. 20 applying another method in the 2D approximation we have estimated that $w_2 = 0.013w_1$. In the present paper these new values of w_2 and w_3 will be used in order to model the thermoelectric properties more precisely.

From Eq. (7) it is seen that, if we put $d_1 = 0$ and $d_2 = 0$, the integrals on η and ζ can be calculated directly and the results of 1D model are obtained. In this case the expression under integral on ε has a maximum at $\varepsilon = \varepsilon_0$, determined by the compensation of both hole-phonon interactions for states near ε_0 , mentioned above. The effect of this maximum determines the possibility to improve the thermoelectric properties of TTT_2I_3 crystals. In the 1D model the maximum is limited by D_0 (the rate of impurity and defects scattering) and may be rather high, if D_0 is sufficiently small. In the 3D model the maximum is limited also by the scattering on adjacent chains. Therefore it is important to determine the criteria when this interaction will predominate and further purification of crystals will not lead to improvement of the thermoelectric properties.

3. Results and discussion

Calculations after (5)-(7) can be made only numerically. The crystal parameters are: $M = 6.5 \times 10^5 m_e$ (m_e is the mass of the free electron), $a = 18.35 \text{ \AA}$, $b = 4.96 \text{ \AA}$, $c = 18.46 \text{ \AA}$, $w_1 = 0.16 \text{ eV}$, $w'_1 = 0.26 \text{ eV \AA}^{-1}$, $v_{s1} = 1.5 \times 10^3 \text{ m/s}$, $E_F = 0.12 \text{ eV}$, $\kappa_{xx}^L = 0.6 \text{ WK}^{-1} \text{m}^{-1}$, $d_1 = d_2 = 0.015$. The polarizability α_0 of TTT molecule in a crystal is not known. Calculation by DFT gives $\alpha_0 = 50 \text{ \AA}^3$ for the TTT molecule in vacuum. It seems that this value is somewhat increased. We have chosen $\alpha_0 = 42 \text{ \AA}^3$ that corresponds to

$\gamma_1 = 1.6$. For this value, $\gamma_2 = \gamma_1 b^5 / (a^5 d_2) = \gamma_3 = 4.3$. A small increase of α_0 will only displace the maximums in Figs. 1, 3, 4 to slightly higher values of Fermi energy.

For the parameter D_0 the following values have been chosen: 0.6 which corresponds to crystals grown from solution with stoichiometric conductivity $1.8 \times 10^5 \Omega^{-1} \text{m}^{-1}$ [17]; 0.09 which corresponds to crystals grown from gaseous phase with stoichiometric conductivity $10^6 \Omega^{-1} \text{m}^{-1}$ [18]; 0.05 which corresponds to crystals grown from gaseous phase with somewhat higher conductivity $1.7 \times 10^6 \Omega^{-1} \text{m}^{-1}$ not synthesized yet.

In Fig.1a the dependences of electrical conductivity σ_{xx} on dimensionless Fermi energy $\varepsilon_F = E_F/2w_1$ are presented. The results of calculations made in the 1D model are presented by red dotted lines and those made in the 3D model – by blue dashed lines. It is seen that for crystals with low degree of purity the curves with low maximum coincide in the whole interval of Fermi energy. For more perfect crystals the curves with mid maximum practically also coincide. Only in the most perfect crystals not synthesized yet (the curves with high maximum) a small deviation is observed, but it is still negligible. The analysis shows that the simplified 1D approximation can be applied for crystals with stoichiometric electrical conductivity up to $\sigma_{xx} \sim 3 \times 10^6 \Omega^{-1} \text{m}^{-1}$. In this case the scattering on impurities and defects predominates. In purer crystals with higher conductivity the scattering on adjacent chains becomes also important and the 3D model must be applied.

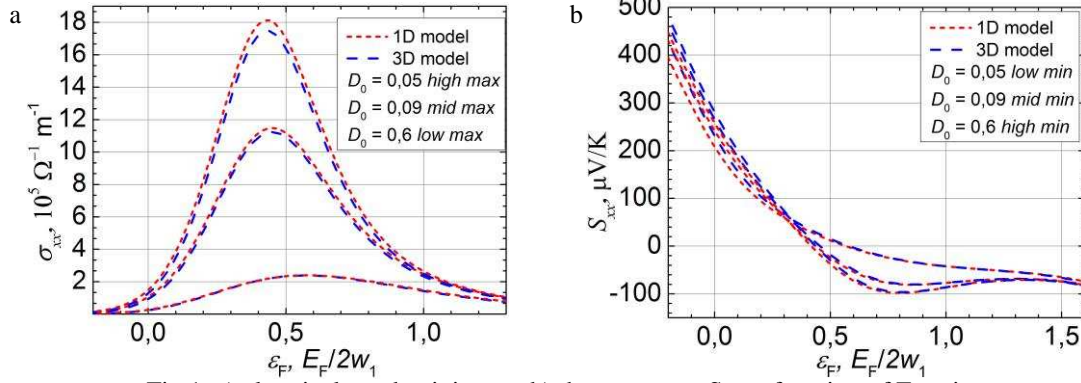


Fig.1. a) electrical conductivity σ_{xx} ; b) thermopower S_{xx} as function of Fermi energy ε_F .

In Fig.1b the dependences of the thermopower (Seebeck coefficient) S_{xx} on dimensionless Fermi energy ε_F are presented. It is seen that the deviations of 3D from the 1D model are also negligible. For stoichiometric crystals ($\varepsilon_F = 0.37$) the values of S_{xx} weakly depend on D_0 and are very close to experimentally observed value $\sim 40 \mu\text{VK}^{-1}$. When ε_F decreases, S_{xx} grows considerably. It is favorable for the increase of ZT.

In Fig.2a the dependences of the electronic thermal conductivity κ_{xx}^e on dimensionless Fermi energy ε_F are presented. The deviations of 3D from the 1D model are also negligible. κ_{xx}^e increases considerably with the increase of crystal purity, but the maximum of κ_{xx}^e is displaced to higher values of ε_F with respect to the maximum of σ_{xx} . This leads to a diminution of the Lorenz number for $\varepsilon_F \sim 0.1 - 0.2$ and is also favorable for the increase of ZT.

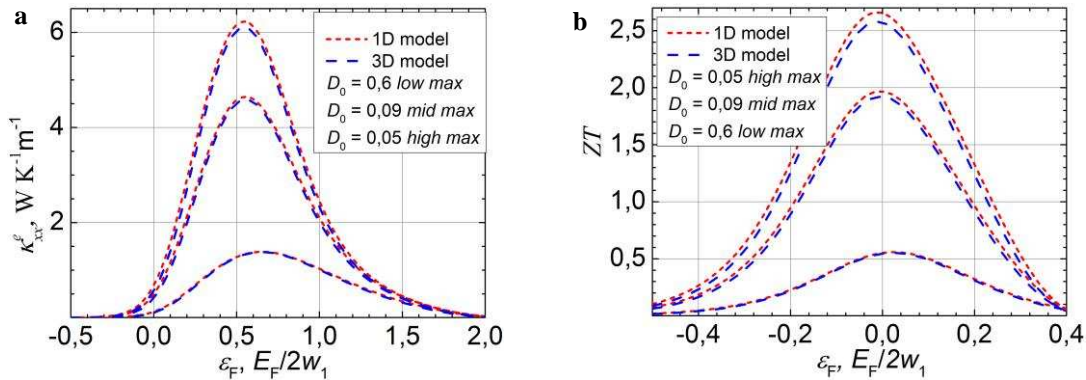


Fig.2. a) electronic thermal conductivity κ_{xx}^e ; b) figure of merit $(ZT)_{xx}$ as function of Fermi energy ε_F .

In Fig.2b the dependences of the thermoelectric figure of merit $(ZT)_{xx}$ on dimensionless Fermi energy ε_F are presented. The deviations of 3D from the 1D model have increased for the purest crystals, but are also negligible. It is seen that in stoichiometric crystals ($\varepsilon_F = 0.37$) the values of $(ZT)_{xx}$ are small, ~ 0.1 even in the crystals with increased electrical conductivity. This is explained by the respective increase of electronic thermal conductivity. In order to increase $(ZT)_{xx}$ it is needed to diminish ε_F , or the carrier concentration. It is seen (curves with mid maximum) that when ε_F is diminished down to 0.12 (or the carrier concentration is diminished from $1.2 \times 10^{27} \text{m}^{-3}$ down to $0.6 \times 10^{27} \text{m}^{-3}$), $(ZT)_{xx}$ is increased up to 1.4 in reported crystals with stoichiometric conductivity $10^6 \Omega^{-1} \text{m}^{-1}$, and even $(ZT)_{xx} = 1.9$ is expected in crystals with somewhat higher conductivity (curves with high maximum). This is favorable for thermoelectric applications of TTT_2I_3 crystals. The tuning of Fermi level to needed value can be achieved by synthesizing non stoichiometric crystals with deficiency of iodine which plays the role of acceptor end

determines the hole concentration in TTT stacks. Crystals of TTT_2I_3 admit nonstoichiometric composition. The 3D and 1D models show small deviation only in not very perfect crystals in which the carrier mobility is limited by the scattering on impurities and defects. The analysis shows that the interchain interaction can be neglected, if the calculated maximum of $(\text{ZT})_{\text{xx}}$ is less than 4. In still more perfect crystals the interchain interaction must be taken into account, because namely this interaction begins to limit the carrier mobility. In this case the 3D crystal model must be applied, so as the deviation between 3D and 1D models will exceed 10%.

4. Conclusions

A more complete 3D physical model for quasi-one-dimensional organic crystals of TTT_2I_3 is developed. In these crystals the carriers are holes. Interactions of holes with longitudinal acoustic phonons determined by the fluctuations of the polarization energy of molecules surrounding the conduction hole and by the fluctuations of the transfer energies for a hole, as well as the interactions with impurities and defects are taken into account, generalized for the 3D case. For the first time the electrical conductivity σ_{xx} , the thermopower (Seebeck coefficient) S_{xx} , the electronic thermal conductivity κ_{xx}^e and the thermoelectric figure of merit $(\text{ZT})_{\text{xx}}$ along the conductive chains have been modelled as function of Fermi energy in the 3D model. It is found that the interchain interaction can be neglected for crystals with stoichiometric electrical conductivity up to $\sigma_{\text{xx}} \sim 3 \times 10^6 \Omega^{-1}\text{m}^{-1}$, or with the calculated maximum of $(\text{ZT})_{\text{xx}}$ less than 4. In this case the scattering on impurities and defects predominates. In purer crystals with higher conductivity the interchain interaction becomes important and the 3D model must be applied. It is also found that $(\text{ZT})_{\text{xx}}$ is increased up to 1.4 in reported crystals with stoichiometric conductivity $10^6 \Omega^{-1}\text{m}^{-1}$, if the carrier concentration is diminished by two times, i.e. from $1.2 \times 10^{27} \text{m}^{-3}$ down to $0.6 \times 10^{27} \text{m}^{-3}$. In this case the expected crystal parameters are: $\sigma_{\text{xx}} = 2.9 \times 10^5 \Omega^{-1}\text{m}^{-1}$, $S_{\text{xx}} = 175 \mu\text{VK}^{-1}$, $\kappa_{\text{xx}}^e = 1.2 \text{WK}^{-1}\text{m}^{-1}$ and $k_{\text{xx}} = 1.8 \text{WK}^{-1}\text{m}^{-1}$. In crystals with somewhat higher stoichiometric conductivity $1.7 \times 10^6 \Omega^{-1}\text{m}^{-1}$ not synthesized yet, $(\text{ZT})_{\text{xx}} = 1.9$ is predicted (instead of 2 in the 2D model). The crystal parameters in this case are: $\sigma_{\text{xx}} = 4.1 \times 10^5 \Omega^{-1}\text{m}^{-1}$, $S_{\text{xx}} = 186 \mu\text{VK}^{-1}$, $\kappa_{\text{xx}}^e = 1.6 \text{WK}^{-1}\text{m}^{-1}$ and $k_{\text{xx}} = 2.2 \text{WK}^{-1}\text{m}^{-1}$. These parameters are quite reasonable.

Acknowledgements

Authors acknowledge the support from EU Commission FP7 program under the grant no. 308768

References

- [1] J Q. Zhang, Y. Sun, W. Xu, and D. Zhu. Adv. Mater. 2014, DOI: 10.1002/adma.201305371.
- [2] G-H. Kim, L. Shao, K. Zhang and K. P. Pipe. Nat. Mater. Vol. 12, 2013, DOI: 10.1038/NMAT3635.
- [3] Park, T., Park, C., Kim, B., Shin, H. & Kim, E. Energy Environ. Sci. 6, 788_792 (2013).
- [4] Y. M. Sun, P. Sheng, C. A. Di, F. Jiao, W. Xu, D. Qiu, D. Zhu, Adv. Mater. 2012, 24, 932.
- [5] O. Bubnova, Z. U. Khan, A. Malti, S. Braun, M. Fahlman, M. Berggren, X. Crispin, Nat. Mater. 2011, 10, 429.
- [6] S. H. Lee, H. Park, S. Kim, W. Son, I. W. Cheong and J. H. Kim. J. Mater. Chem. A, 2014, 2, 7288.
- [7] N. E. Coates, S. K. Yee, B. McCulloch, K. C. See, A. Majumdar, R. A. Segalman, Jeffrey, J. Urban, Adv. Mater. 2013, 25, 1629.
- [8] W. Q. Ao, L. Wang, J. Q. Li, Fred Pan, C. N. Wu. JEM, 40, 2027 (2011).
- [9] Jihui Yang, Hin-Lap Yip, Alex K.-Y. Jen. Advanced Energy Materials, 3, 549 (2013).
- [10] Shane P. Ashby, Jorge García-Cañadas, Gao Min & Yimin Chao, JEM, 42, 1495 (2013).
- [11] G. Kim, K. P. Pipe. Phys. Rev. B, 86, 085208 (2012).
- [12] J. Chen, D. Wang, Z. Shuai, J. Chem. Theory Comput., 8 (9), 3338 (2012) DOI: 10.1021/ct3004436.
- [13] Zheyong Fan, Hui-Qiong Wang, and Jin-Cheng Zheng. J. Appl. Phys., 109, 073713 (2011).
- [14] D. Wang, L. Tang, M. Long, and Z. Shuai. J. Phys. Chem. C, 115 (13), 5940, (2011). DOI: 10.1021/jp108739c.
- [15] Y. Wang, J. Zhou, and R. Yang. J. Phys. Chem. C, 115, 24418 (2011).
- [16] A. Casian, in: Thermoelectric Handbook, Macro to Nano, Ed. by D. M. Rowe, CRC Press, 2006, Chap.36.
- [17] V.F. Kaminskii, M.L. Khidekel', R.B. Lyubovskii and oth. Phys. Status Solidi A 44, 77 (1977).
- [18] Hilti B. and Mayer C.W. Helvetica Chimica Acta, 61, Nr 40, 501, (1978).
- [19] A. Casian, I. Sanduleac. JEM, 2014, DOI: 10.1007/s11664-014-3105-6.